July 2005

# Deconvolution of the $Co_3O_4(110)$ Fuchs–Kliewer phonon spectrum

E.M. Marsh
*University of Nebraska - Lincoln*

S.C. Petitto
*University of Nebraska - Lincoln*

G.S. Harbison
*University of Nebraska - Lincoln*

K.W. Wulser
*University of Nebraska - Lincoln*

Marjorie Langell
*University of Nebraska - Lincoln*, mlangell1@unl.edu

# Deconvolution of the $Co_3O_4(110)$ Fuchs–Kliewer phonon spectrum

E. M. Marsh, S. C. Petitto, G. S. Harbison, K. W. Wulser, and M. A. Langell[a)]
*Department of Chemistry, University of Nebraska, Lincoln, Nebraska 68588-0304*

(Received 1 October 2004; accepted 3 January 2005; published 28 June 2005)

The Fuchs–Kliewer phonon spectrum of single crystal $Co_3O_4(110)$ has been treated with a Fourier transform log deconvolution method, which removes multiple scattering features from the single loss spectrum. Auger electron spectroscopy (AES), x-ray photoelectron spectroscopy (XPS) and low-energy electron diffraction (LEED) were first used to characterize the $Co_3O_4$ crystal establishing the cleanliness, composition, and order of the (110) surface. High resolution electron energy loss spectroscopy (HREELS) was then used to obtain the phonon spectrum for an incident electron energy of 3.77 eV. Due to the strong dipole cross section for the Fuchs–Kliewer phonon modes, intense multiple electron scattering was detected, which provided a complicated and overlapping combination of all possible loss modes. Deconvolution removed the multiple loss modes to produce well-resolved Fuchs–Kliewer fundamental phonon losses at 218, 373, 598, and 682 $cm^{-1}$ (27.0, 46.2, 74.1, and 84.6 meV). These values are compared to the fundamental loss energies obtained by resolving the overlapping peak structure with standard peak fitting procedures, which confirmed the single loss energies obtained with the deconvolution procedure. Deconvolution results from the four fundamental phonon spectrum of single crystal $Co_3O_4(110)$ were also compared to those from the simpler spectra of CoO(100) and thin-film CoO(100)–$Co_3O_4$ epitaxy and some practical aspects of the deconvolution process discussed in this context. © *2005 American Vacuum Society.* [DOI: 10.1116/1.1863972]

## I. INTRODUCTION

The transverse optical vibrational modes of transition metal oxides (TMO) are known to produce an intense series of vibrational losses in their high resolution electron energy loss (HREEL) spectrum.[1–4] Known as Fuchs–Kliewer phonons, the normal loss modes for these materials have substantial dipolar scattering cross sections due to the collective, out of phase cation and anion oscillations. HREELS obtained on TMO surfaces, therefore, typically exhibit extensive multiple-loss scattering, and the Fuchs–Kliewer phonon spectrum can easily dominate the TMO HREEL spectrum when obtained in the specular (dipole-dominant) direction. Because the scattering events are uncoupled, the multiple scattering is statistical and the *n*-fold losses decrease in a Poisson distribution that is well-described by classical dielectric theory.[1,5,6]

Although the Fuchs–Kliewer phenomenon has been known and understood for TMOs for approximately 30 years,[7] most reported TMO HREEL spectra have been performed on only a handful of materials, most notably MgO,[8–10] NiO,[11–14] $TiO_2$,[15–17] $SrTiO_3$[18] and $Al_2O_3$,[10,19–21] both in thin film and in crystalline form. In the majority of these studies, the phonon spectrum was considered a nuisance to be eliminated, or at least minimized, in order to free the HREEL spectral range and allow detection of adsorbate vibrational losses. The collective phonon loss features can be hundreds of times more intense than losses resulting from localized adsorbate modes, and the Fuchs–Kliewer phonon spectrum can obscure the adsorbate losses completely. Even studies focusing on the phonon spectrum found that for low-symmetry TMOs the multiple loss structure made it difficult to resolve all fundamental loss modes from poorly resolved, overlapping multiple loss structure. Unfortunately, many of the TMOs do not conduct well and the broad nature of their HREEL spectra due to surface charging effects exacerbates the problem.

The cobalt oxide TMO $Co_3O_4$ is a spinel with four fundamental phonon modes, which have previously been identified by IR/Raman[22,23] and computational[22] methods. The crystal structure can be related to the simpler, rocksalt monoxide, CoO, through the symmetrically equivalent lattice oxide structure of closest packed fcc $O^{2-}$. The spinel and rocksalt differ primarily in the site occupation of the cobalt ions. While CoO has a single type of $Co^{2+}$ ions in every available octahedral site, the spinel has $Co^{3+}$ ions occupying one half of the available octahedral sites and $Co^{2+}$ ions occupying one eighth of the available tetrahedral sites, reducing the symmetry from $Fm\bar{3}$ m to $Fd\bar{3}$ m and increasing the number of fundamental phonons from one to four. With four fundamental phonons and all multiple scattering combinations of the modes, the spinel has a significantly more complicated loss spectrum. For this reason it would be useful to have a deconvolution procedure that can be applied to the spectra to eliminate or substantially reduce the intensity from the multiple loss phonons but at the same time preserve any adsorbate losses that might be present in the HREEL spectrum. A simple, yet effective, Fourier log deconvolution algorithm was first demonstrated for NiO(100) and $SrTiO_3(100)$ Fuchs–Kliewer phonons by Cox *et al.* for the removal of multiple loss scattering features in the HREEL spectra.[24]

a)Author to whom correspondence should be addressed; electronic mail: mlangell@unlserve.unl.edu

Loss features result from all possible multiple scattering events including both $n$-fold losses of each of the fundamental modes as well as all multiple-loss combinations among them. For uncorrelated multiple scattering events, spectral intensities are expected to vary as the convolute[24]:

$$s(\omega) = i(\omega) \otimes \left\{ \delta(0) + p(\omega) + \frac{1}{2!}p(\omega) \otimes p(\omega) + \frac{1}{3!}p(\omega) \otimes p(\omega) \otimes p(\omega) + \cdots \right\}, \quad (1)$$

where $s(\omega)$ is the Fuchs–Kliewer single-loss phonon spectrum of the fundamental loss modes, $i(\omega)$ is the instrument response function, $\otimes$ represents a mathematical convolute, $\delta(0)$ is a delta function that, when convoluted with the spectrometer function, creates the elastic peak shape, and $p_i(\omega)$ represents the single loss phonon spectrum of the $i$th fundamental mode. Upon taking the Fourier transform of the function, convoluted, multiple scattering effects become simple products:

$$S(\tau) = I(\tau)\left[ 1 + P(\tau) + \frac{1}{2!}P(\tau)^2 + \frac{1}{3!}P(\tau)^3 + \cdots \right]. \quad (2)$$

The bracketed term is essentially the expansion of the $e^{p(t)}$, and $P(t)$ can be obtained after removal of the instrument response function by taking the natural log of the function:

$$P(t) = \log_e[S(t)/I(t)]. \quad (3)$$

By back transforming Eq. (3), it is possible to remove multiple loss scattering contributions:

$$I(t)\log_e[S(t)/I(t)] \leftrightarrow p(w) \times i(w). \quad (4)$$

In this paper, we apply this log deconvolution to $Co_3O_4$(110) HREELS Fuchs–Kliewer phonon data to resolve clearly the fundamental loss modes. We compare the results to simple peak-fit spectra[25] and to literature IR/Raman data.[22,23]

## II. EXPERIMENT

$Co_3O_4$ single crystals were grown from a molybdate electrolytic flux and exhibited the expected truncated octahedron morphology with naturally occurring (110) and (111) faces. For this study, a crystal with a well defined (110) face measuring 2 mm $\times$ 3 mm was chosen. Gold foil was used to wrap the sample leaving only the (110) face exposed and tantalum wires, capable of providing resistive heating up to 1000 K, were wrapped around the sample and attached to two heating posts suspending the sample between them. A Chromel–Alumel thermocouple spot-welded to the gold foil on the back of the sample allows for temperature monitoring.

A stainless steel ultra high vacuum (UHV) chamber with an operating base pressure of approximately $3.0 \times 10^{-8}$ Pa houses the instruments used to conduct the surface sensitive experiments. Cleaning cycles of $Ar^+$ sputtering ($4 \times 10^{-3}$ Pa $Ar^+$, 2.3 $\mu A/cm^2$) for 30 min at 300 K, annealing under $O_2$ ($1.3 \times 10^{-5}$ Pa) for 20 min at 630 K, and annealing under UHV for 10 min at 630 K removed impurities present on the air exposed sample. The cycle was repeated until the $Co_3O_4$(110) surface appeared free from impurities in the Auger electron spectra and stoichiometric by Auger electron spectroscopy (AES) and x-ray photoelectron spectroscopy (XPS).

Single crystal CoO(100) was grown from the flame fusion method by Atomergic Chemetals Corp. and using back Laue diffraction were oriented to within 0.5° of the (100) plane. The CoO(100) was subjected to repeated *in situ* cleaning cycle of $Ar^+$ bombardment, $O_2$ annealing, and UHV annealing until the crystal showed no impurities by AES. Thin films of $Co_3O_4$ were grown epitaxially on the CoO(100) surface by oxidation from extended exposure to $O_2$ at 625 K. The crystal has previously undergone characterization by AES, XPS, LEED, and HREELS and more details about the preparation and characterization can be found elsewhere.[26]

Both AE and XP spectra were collected using a Physical Electronics ($\Phi$) 15–255 G double-pass cylindrical mirror analyzer (DPCMA). A primary beam energy of 2 kV with a resolution of 1 eV/step and a scan rate of 20 eV/s was used to acquire the AE spectra and are taken in an $N(E)$ vs. E mode. XP spectra were collected using MgK$\alpha$ (hv = 1253.6 eV) or AlK$\alpha$ (hv = 1468.6 eV) as a radiation source with a resolution of 0.1 eV/step at 200 ms/step, a constant pass energy of 25 eV and 100 scan signal averaging.

Low-energy electron diffraction (LEED) data showed the $Co_3O_4$(110) crystal to be well ordered. The LEED data were acquired at 300 K over an energy range from 30 to 150 eV using a Vacuum Generator 8011 rear view four grid LEED optics. An EE2000 SMARTOOL software package was used to record and analyze the diffraction patterns.

HREELS experiments were conducted using a LK2000 double pass 127° electron energy analyzer at 300 K. The primary electron beam impinges the sample at an angle 60° relative to the surface normal and data were taken in the specular mode. For well-ordered metal surfaces, spectrometer resolution can typically be obtained at 3–5 meV, however the poorly conducting nature of the metal oxide spinel has decreased the resolution to approximately 15 meV as measured from the full width at half maximum (FWHM) of the elastic peak. The primary beam energy for spectra reported here is 3.77 eV, although comparable information was obtained from data taken over the range of 2.25–14.25 eV, which are reported elsewhere.[25] The HREELS data were curve fit using PEAKFIT V4 software and the Pearson IV peak function available in the PEAKFIT package.[27] The Pearson IV function was chosen because of its ability to match asymmetric peak shapes and spectral tailing to best approximate the HREELS data. Deconvolution of the HREELS data was implemented with MATHEMATICA V5.0[28] using standard Gaussian and Lorentzian line shapes available with the software to reproduce the instrument response function and the built-in discrete Fourier transform to effect the log deconvolution.

## III. DATA

XP spectra of the O 1$s$ and Co 2$p$ peaks for the clean, stoichiometric $Co_3O_4$(110) surface are shown in Fig. 1, and

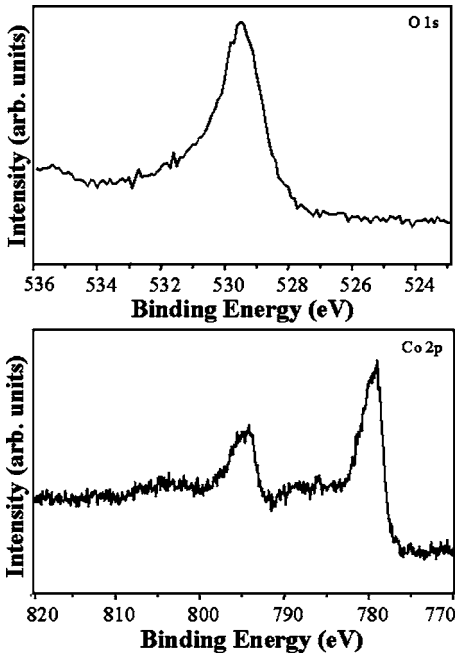


FIG. 1. XPS spectra of the O 1*s* region and the Co 2*p* region for the $Co_3O_4$(110) spinel substrate. Data are taken at 25 eV pass energy with MgK$\alpha$ radation.

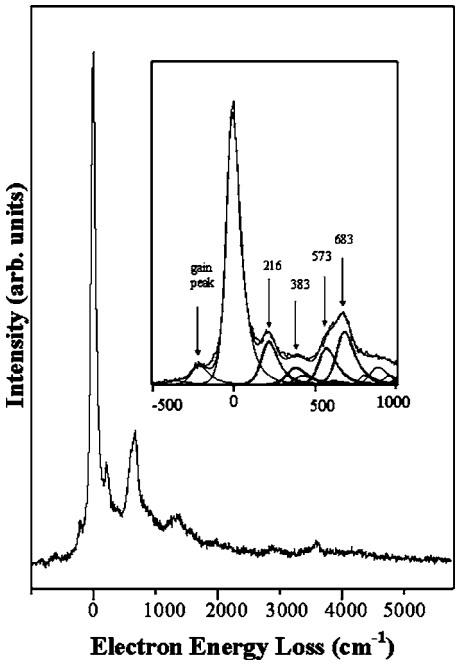


FIG. 3. HREELS of the Fuchs–Kliewer phonon spectrum taken with a primary beam energy of 3.77 eV for the $Co_3O_4$(110) substrate. The single loss region is shown in the inset, with peaks fit to fundamental frequencies and multiple losses that occur in this region. The bold lines represent the fit peaks for single losses of the four fundamental peaks and the other peaks are fit peaks for a gain peak and the second losses of the four fundamental phonons that fall in this energy region.

are comparable to literature data for the spinel oxide both in binding energies and peak shapes.[29–40] The O 1*s* peak is found at 529.6 eV, and the hydroxyl impurity surface concentration can be estimated to be $\leqslant$10% by fitting the tailed peak structure of the O 1*s* spectrum. Cobalt $2p_{3/2}$ and $2p_{1/2}$ are found at 779.8 and 795.7 eV, respectively, and the weak satellites at approximately 788.8 and 804.2 eV are characteristic of a well-oxidized $Co_3O_4$ surface. Carbon impurities were at or below detection limits in broad scan (0–1000 eV) XPS and in AES, and relative peak intensities were within error of the expected stoichiometric O/Co ratios. Figure 2 shows a typical $Co_3O_4$(110) LEED photograph, taken at 147 eV, with a sharp rectangular pattern that confirms the well-ordered structure of the cubic spinel (110) surface.[29]

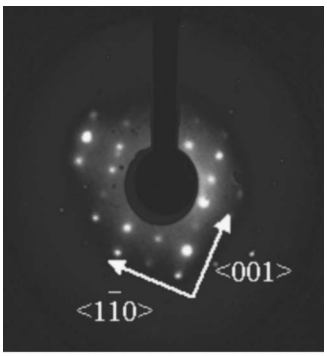


FIG. 2. LEED photograph showing the well ordered $Co_3O_4$(110) surface taken with a beam energy of 147 eV.

A representative Fuchs–Kliewer phonon spectrum for the $Co_3O_4$(110) substrate is shown in Fig. 3. The intense and long range nature of dipole scattering from the Fuchs–Kliewer phonons creates multiple scattering events producing loss spectra that include the *n*-fold loss features of each fundamental phonon along with every possible multiple-loss combination among them. Due to the complexity of the loss spectra, the PEAKFIT V4 software package was used to resolve the individual phonon losses by fitting with a Pearson IV peak shape,[27] which is capable of simulating the asymmetric and tailing characteristics of the phonon spectrum. The inset to Fig. 3 shows a detailed view of the fitted single loss region and assigns loss energies of 216, 383, 573, and $683 \pm 15.8$ cm$^{-1}$ (26.8, 47.5, 71.1, and 84.7, $\pm$2.0 meV) to the four fundamental phonons. These values are within error of infrared (IR) and computational values found in the literature.[22,23] More detail about the characterization and fitting procedure used to resolve this phonon spectrum is reported elsewhere.[25]

The HREEL spectra for CoO(100) and CoO(100)–$Co_3O_4$(100) are shown here for comparison to the $Co_3O_4$(110) data (Fig. 4). Because of the symmetric nature of the CoO crystal structure, there is a single fundamental Fuchs–Kliewer phonon mode. The multiple loss peaks are fairly well resolved from each other and occur predictably at integral values of the fundamental loss mode. The (100) surface is the thermodynamically favored orientation for rocksalt monoxides and is substantially more stable than other, polar faces. Because (100) is not a preferred orientation for $Co_3O_4$, the epitaxy

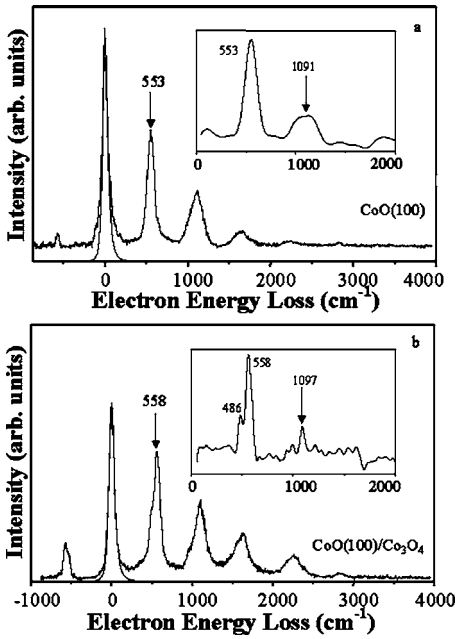


FIG. 4. Fuchs–Kliewer phonon spectra of (a) CoO(100) and (b) CoO(100)–$Co_3O_4$ surfaces. The insets show the deconvolution of the spectra by the Fourier transform log process.

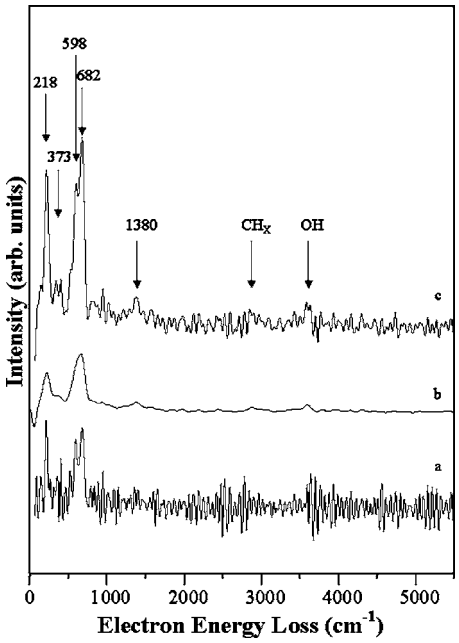


FIG. 5. Deconvolution of the $Co_3O_4$(110) HREEL spectrum using the Fourier transform log deconvolution process. Each series represents a different amount of Gaussian–Lorentzian windowing: (a) Shows the deconvolution using the best fit to the elastic peak, (b) is the deconvolution followed by a Gaussian smoothing using the function $\exp -\nu^2/\sigma$ with a broadening factor $\sigma=8.48\times10^{-4}$ $(cm^{-1})^{-2}$, (c) shows the deconvolution followed by Gaussian smoothing at $\sigma=2.57\times10^{-4}$ $(cm^{-1})^{-2}$ and an exponential line narrowing function in the Fourier conjugate domain of $\exp[(\nu)^{-1}\lambda$. with $\lambda=75.5$ $cm^{-1}]$.

only grows to 5–10 layers before saturating under the UHV growth conditions used. Thus, its contribution to the HREEL spectrum is weak and the CoO(100)– $Co_3O_4$ (100) spectrum is dominated by the CoO(100) substrate. Normal mode loss energies do not depend upon surface orientation, and while some intensity variation might result as a function of substrate orientation, the phonons are fairly long range in nature. Thus, while the $Co_3O_4$ epitaxy forms with (100) orientation on the CoO(100) substrate, the loss positions should be comparable to those of $Co_3O_4$(110) if the epitaxy is truly characteristic of the $Co_3O_4$ substrate.

The elastic peaks of the CoO(100) and CoO(100)–$Co_3O_4$ (100) spectra were fit with the PEAKFIT V4 software and the Pearson IV peak shape to obtain an estimate for the instrument response function, which was then Fourier transformed and used in the deconvolution process as described in Eq. (3). After deconvolution, the CoO(100) spectrum produces a peak at 553 $cm^{-1}$ (68.6 meV) that corresponds very well to the fundamental phonon loss energy expected for the CoO rocksalt structure.[26] The CoO(100)–$Co_3O_4$ (100) HREEL spectrum is also dominated by this peak, but the spectrum now indicates reduced structural symmetry through the appearance of a new peak at 486 $cm^{-1}$ (60.3 meV). Both spectra also show a small $O_2$ adsorbate peak at 1091 $cm^{-1}$ (135.3 meV ) as a result of the trapping of $O_2$ in surface annealing during cleaning or in the formation of the $Co_3O_4$ epitaxy.[41,42] This adsorbate could not be easily detected in the raw data without aid of the deconvolution and would not have been apparent from simple curve fitting of the spectrum. While the thin film epitaxy does show reduced symmetry from CoO, it does not yet show the expected phonon spectrum of the well-developed bulk $Co_3O_4$ structure.

Figure 5 depicts the deconvolution of the single crystal $Co_3O_4$(110) Fuchs–Kliewer phonon spectrum as a function of choice for the instrument response function. Because of noise and the tailing background from secondary electron losses, the instrument response function cannot be known precisely, and is approximated by fitting the elastic peak with a tailed Gaussian–Lorentzian function. Figure 5(a) provides an example of the deconvolution process using the best fit to the elastic peak. Unfortunately, this approach does not give good results and does not present sufficient signal to noise to identify the four fundamental loss modes of the $Co_3O_4$(110) Fuchs–Kliewer phonon spectrum. This is a common problem in Fourier deconvolution of noisy data and is exacerbated by the need to take the log of small, noisy signals [Eq. (3)] at large times in the Fourier domain.

Additional smoothing can improve Fourier analysis of noisy data, and this is effected for HREELS data in the Fourier time domain by multiplication of a Gaussian peak slightly wider than the instrument response function. The wider the Gaussian, the more severe the smoothing and the poorer the resolution. Figure 5(b) shows deconvolution followed by Gaussian smoothing using the function $\exp -\nu^2/\sigma$ with a broadening factor $\sigma=8.48\times10^{-4}(cm^{-1})^{-2}$. This is the approach taken above for the relatively simple spectra for CoO(100) and CoO(100)–$Co_3O_4$(100) epitaxy in Fig. 4 and gives adequate results. Gaussian smoothing gives a better signal to noise ratio for the $Co_3O_4$(110) single crystal phonon spectrum, however, the peaks have been broadened to

the point where it is impossible to identify all four fundamental phonons in the $Co_3O_4$(110) spectrum [Fig. 5(b)].

The spectrum can be sharpened by using a narrower instrument response function, but only at the expense of added noise that obscures weak features. However, Fourier analysis allows advantage to be taken in the differences between Lorentzian and Gaussian peak shapes.[43] Lorentzian line shapes are broader close to the baseline, and by removing the Lorentzian component of the spectrum and replacing it with Gaussian character, the noise can be kept sufficiently low but the resolution at the baseline improved to allow for small peaks to be detected. Figure 5(c) shows the Gauss–Lorentz resolution enhanced spectrum, obtained with Gaussian smoothing at $\sigma=2.57\times10^{-4}$ $(\mathrm{cm}^{-1})^{-2}$ and an exponential line narrowing function in the Fourier conjugate domain of $\exp[(\nu)^{-1}\lambda.$ with $\lambda=75.5$ $\mathrm{cm}^{-1}]$. Here the fundamental phonon peaks have been sharpened without compromising the signal to noise ratio, and particularly the two high-energy phonons are now resolved. The loss peaks were observed at 218, 373, 598, and 682 $\mathrm{cm}^{-1}$ (27.0, 46.2, 74.1, and 84.6 meV). The weakest phonon peak at 373 $\mathrm{cm}^{-1}$ is unfortunately, just slightly greater than the noise level and is most strongly affected by the baseline noise.

From the $Co_3O_4$(110) HREEL spectrum after deconvolution, it is also possible to identify several small adsorbate peaks. These peaks are very weak and are just at or below detection levels in AES and XPS, indicating they are at submonolayer levels. The 3600 $\mathrm{cm}^{-1}$ peak is due to surface hydroxyls, which may have been present at low levels of $\leqslant$10% relative to the lattice oxygen in the O 1*s* XPS spectrum, just at the limit of XPS for resolving this peak in the spectrometer used. The 2880 $\mathrm{cm}^{-1}$ peak is due to $CH_x$ type adsorbates, which form over the time required to position and focus the sample in the HREEL spectrometer and to acquire the HREELS data. It was not detected by XPS analysis taken on the $Co_3O_4$(110) substrate after the HREELS experiments were conducted.

The remaining peak, at 1380 $\mathrm{cm}^{-1}$, does not present a unique assignment and cannot be unambiguously identified at the present time. Several common impurities can be ruled out. The loss energy is too high to be indicative of adsorbed $O_2^-$ at approximately 1100 $\mathrm{cm}^{-1}$,[41,42] as was observed to result from oxygen annealing on the CoO(100) and CoO(100)–$Co_3O_4$(100) epitaxy samples. It is also too low to be associated with the scissoring mode of molecularly adsorbed water, at about 1600 $\mathrm{cm}^{-1}$,[44] which might be expected to adsorb from the UHV ambient. Carbonate adsorbate losses are found in this region, but the other normal modes expected from carbonate species[45] are not detected. We tentatively assign this peak to a lattice oxygen defect, perhaps a terminal oxygen species as has previously been observed for polar $Cr_2O_3$.[46] Another possibility is that the peak results from a true overtone, which most closely matches that from the P4 fundamental mode ($2\times682=1364$ $\mathrm{cm}^{-1}$). A final possibility offered at this time is that the feature results from incomplete removal of the Fuchs–Kliewer multiple loss structure, a result of not knowing the instrument response function or otherwise improperly reproducing the tailed nature of the data. These possibilities are under active investigation.

## IV. CONCLUSION

Single crystal $Co_3O_4$(110) has been analyzed for surface integrity by AES, XPS and LEED and its Fuchs–Kliewer phonon spectrum obtained by high resolution electron energy loss spectroscopy. Because of multiple scattering effects, the phonon spectrum is difficult to resolve. The spectrum was deconvoluted to remove multiple scattering effects and the four fundamental phonons were obtained at 218, 373, 598, and 682 $\mathrm{cm}^{-1}$ (27.0, 46.2, 74.1, and 84.6 meV) in good agreement with literature IR data and with peak-fitting results previously published for this surface. Better resolution can be obtained by deconvoluting the Lorentzian component of the HREELS line shape, at the expense of greater noise. This can be somewhat ameliorated by replacing the Lorentzian component with a Gaussian line shape.

The deconvoluted spectrum was also compared to that obtained on the CoO(100) surface, which is much simpler in that the higher symmetry rocksalt structure has only a single fundamental phonon mode, and an epitaxial film of CoO(100)–$Co_3O_4$, which only exhibits weak phonon structure from the $Co_3O_4$ overlayer and is otherwise dominated by the simpler CoO Fuchs–Kliewer spectrum resulting from a single fundamental loss mode.

The deconvolution approach clearly shows the presence of adsorbates on the surface, which form during the time required for positioning and focusing the HREELS and for acquiring the data. The adsorbate peaks are more apparent in the deconvoluted spectrum, for example the $O_2^-$ peak at 1091 $\mathrm{cm}^{-1}$ peak, which results under oxygen annealing conditions for CoO(100) and CoO(100)–$Co_3O_4$ epitaxial substrates, would have been missed without deconvolution since it overlaps with the multiple loss structure.

## ACKNOWLEDGMENTS

The authors are grateful for support from the National Science Foundation under Grant No. CHE-0213320 and the University of Nebraska Center for Materials Research and Analysis.

[1] H. Ibach and D. L. Mills, *Electron Energy Loss Spectroscopy and Surface Vibrations* (Academic, New York, 1982).
[2] R. G. Egdell, Stud. Surf. Sci. Catal. **21**, 173 (1985).
[3] B. E. Hayden, Chem. Phys. Solid Surf. **9**, 514 (2001).
[4] M. C. Wu, C. Truong, and D. W. Goodman, Springer Ser. Surf. Sci. **33**, 230 (1993).
[5] P. Lambin, L. Henrard, P. Thiry, C. Silien, and J. P. Vigneron, J. Electron Spectrosc. Relat. Phenom. **129**, 281 (2003).
[6] P. A. Cox and J. P. Kemp, Surf. Sci. **210**, 225 (1989).
[7] H. Ibach, Phys. Rev. Lett. **24**, 1416 (1970).
[8] W. T. Petrie and J. M. Vohs, Surf. Sci. **259**, L750 (1991).
[9] Y. Yu, Q. Guo, S. Liu, E. Wang, and P. J. Moller, Phys. Rev. B **68**, 115414 (2003).
[10] S. C. Street, Q. Guo, C. Xu, and D. W. Goodman, J. Phys. Chem. **100**, 17599 (1996).
[11] G. A. Carson, M. H. Nassir, K. W. Wulser, and M. A. Langell, Surf. Sci. Spectra **5**, 229 (1998).
[12] C. Xu and D. W. Goodman, Catal. Today **28**, 297 (1996).
[13] M. A. Langell and M. H. Nassir, J. Phys. Chem. **99**, 4162 (1995).

[14]M. A. Langell, C. L. Berrie, M. H. Nassir, and K. W. Wulser, Surf. Sci. **320**, 25 (1994).
[15]Z. Chang and G. Thornton, Surf. Sci. **462**, 68 (2000).
[16]M. A. Henderson, S. Otero-Tapia, and M. E. Castro, Faraday Discuss. **114**, 313 (1999).
[17]L. L. Kesmodel, J. A. Gates, and Y. W. Chung, Phys. Rev. B **23**, 489 (1981).
[18]P. A. Cox, R. G. Egdell, and P. D. Naylor, J. Electron Spectrosc. Relat. Phenom. **29**, 247 (1983).
[19]K. A. Layman, M. M. Ivey, and J. C. Hemminger, J. Phys. Chem. B **107**, 8538 (2003).
[20]Z. Jiang, W. Huang, J. Jiao, H. Zhao, D. Tan, R. B. Dali Zhai, and B. Xinhe, Appl. Surf. Sci. **229**, 43 (2004).
[21]Y. Jeliazova and R. Franchy, Appl. Surf. Sci. **187**, 51 (2002).
[22]H. Shirai, Y. Morioka, and I. Nakagawa, J. Phys. Soc. Jpn. **51**, 592 (1982).
[23]M. Lenglet and B. Lefez, Solid State Commun. **98**, 689 (1996).
[24]P. A. Cox, W. R. Flavell, A. A. Williams, and R. G. Egdell, Surf. Sci. **152/153**, 784 (1985).
[25]E. M. Malone, S. C. Petitto, and M. A. Langell, Solid State Commun. **130**, 571 (2004).
[26]M. H. Nassir and M. A. Langell, Solid State Commun. **92**, 791 (1994).
[27]R. E. Brown, PEAKFIT v4.12 Analysis Software Reference, SeaSolve Software Inc., Framingham, MA, 2003.
[28]S. Wolfram *et al.*, MATHEMATICA v5.0, Wolfram Research, Inc., Champaign, IL, 2003.
[29]S. C. Petitto and M. A. Langell, J. Vac. Sci. Technol. A **22**(4), 1690 (2004).
[30]B. A. Sexton, A. E. Hughes, and T. W. Turney, J. Catal. **97**, 390 (1986).
[31]S. Angelov, G. Tyuliev, and T. Marinova, Appl. Surf. Sci. **27**, 318 (1987).
[32]S. Angelov, D. Mechandjiev, B. Piperopv, V. Zarkov, A. Terlecki-Baricevic, D. Jovanovic, and Z. Jovanovic, Appl. Catal. **16**, 431 (1985).
[33]J. L. Gautier, R. Rios, M. Garcia, J. F. Marco, and J. R. Gancedo, Thin Solid Films **331**, 51 (1997).
[34]J. G. Kim, D. L. Pugmire, D. Battaglia, and M. A. Langell, Appl. Surf. Sci. **165**, 70 (2000).
[35]G. A. Carson, M. H. Nassir, and M. A. Langell, J. Vac. Sci. Technol. A **14**, 9006 (1996).
[36]T. J. Chuang, C. R. Brundle, and D. W. Rice, Surf. Sci. **59**, 413 (1976).
[37]J. van Elp, J. L. Wieland, H. Eskes, P. Kuiper, G. A. Sawatasky, R. M. F. de Groot, and T. S. Turner, Phys. Rev. B **44**, 6090 (1991).
[38]M. Oku and Y. Sato, Appl. Surf. Sci. **55**, 37 (1992).
[39]M. A. Langell, C. W. Hutchings, G. A. Carson, and M. H. Nassir, J. Vac. Sci. Technol. A **14**, 1656 (1996).
[40]N. S. McIntyre and M. G. Cook, Anal. Chem. **47**, 2208 (1975).
[41]C. Descorme, Y. Madier, and D. Duprez, J. Catal. **196**, 167 (2000).
[42]B. W. Lee, A. Ignatiev, J. A. Taylor, and J. W. Rabalian, Solid State Commun. **33**, 1205 (1980).
[43]A. G. Ferrige and J. C. Lindon, J. Magn. Reson. (1969-1992) **31**(2), 337 (1978).
[44]P. A. Thiel and T. E. Madey, Surf. Sci. Rep. **7**, 211 (1987).
[45]A. Holmgren, B. Andersson, and D. Duprez, Appl. Catal., B **22**, 215 (1999).
[46]S. Chambers, *The Chemical Physics of Solid Surfaces*, edited by D. P. Woodruff (Elsevier Science, Amsterdam, 2001), Vol. 9, p. 301.